Phytochemistry 199 (2022) 113183

Contents lists available at ScienceDirect

Phytochemistry

journal homepage: www.elsevier.com/locate/phytochem

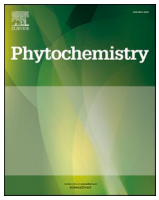

Ingadosides A-C, acacic acid-type saponins from *Inga sapindoides* with potent inhibitory activity against downy mildew☆

Ming Yuan Heng [a], Barbara Thuerig [b], Ombeline Danton [a], Justine Ramseyer [a], Mahabir P. Gupta [c], Lucius Tamm [b], Matthias Hamburger [a], Olivier Potterat [a,*]

[a] Division of Pharmaceutical Biology, Department of Pharmaceutical Sciences, University of Basel, Klingelbergstrasse 50, 4056, Basel, Switzerland
[b] Research Institute of Organic Agriculture FiBL, Ackerstrasse 113, 5070, Frick, Switzerland
[c] Center for Pharmacognostic Research on Panamanian Flora, Faculty of Pharmacy, University of Panama City, Panama

ARTICLE INFO

Keywords:
Inga sapindoides
Fabaceae
Plasmopara viticola
Antifungal activity
Saponins
Ingadosides A-C

ABSTRACT

As part of a project aiming at the discovery of environmentally friendly alternatives to copper in organic agriculture, a 96% ethanolic extract from the leaves of *Inga sapindoides* showed potent inhibitory activity against grapevine downy mildew (*Plasmopara viticola*) *in vitro* (MIC_{100} 25 μg/mL). Separation of the *n*-BuOH soluble fraction by silica gel column chromatography followed by a combination of RP_{18} and HILIC HPLC resulted in the isolation of a series of bidesmosidic saponins characterized by the presence of a monoterpenoid unit attached to a triterpenoid aglycone, a *p*-methoxycinnamoyl residue, and rare sugar residues such as N-acetyl-D-glucosamine, D-quinovose, and D-fucose. The isolated compounds inhibited the formation or activity of *P. viticola* zoospores with MIC_{100} values of 3 or 6 μg/mL, respectively. *I. sapindoides*, a tree which is often cultivated for shading coffee plantations in Central America, may represent a sustainable source of fungicidal products to be used in the replacement of copper.

1. Introduction

Grapevine downy mildew (*Plasmopara viticola* (Berk. & M.A. Curtis) Berl. & De Toni) is a devastating disease in susceptible grapevine cultivars which, therefore, require significant crop protection treatments (Wilcox et al., 2015). Copper-based fungicides have been discovered in the early 1900s, and are still widely used today in conventional, integrated and organic agriculture to control grapevine downy mildew and many other plant diseases (Lamichhane et al., 2018). The maximal allowed amounts of copper have been drastically reduced over the years, but repeated applications can still lead to copper accumulation in the soil, with potential negative impacts on non-target soil organisms (Küpper et al., 2009; Napoli et al., 2019). This has prompted the search for alternatives, such as natural products (Dagostin et al., 2011). These are more environmentally friendly because they typically degrade rapidly under normal field conditions (Street, 1980; Zulkifly et al., 2010). In a collaborative project aiming at the discovery of possible substitutes for copper-based agrochemicals, we screened an in-house library of 3500 plant and fungal extracts for their inhibitory activity against *P. viticola*. As one of the hits, a MeOH extract from the leaves of *Inga sapindoides* Willd. (Fabaceae) led to a complete inhibition of *P. viticola* zoospores at 50 μg/mL *in vitro*, and reduced the leaf area infected by *P. viticola* on grapevine seedlings by 98% at 1 mg/mL.

The genus *Inga* comprises approx. 380 species and consists of tropical trees and shrubs growing in Central and South America. Most phytochemical investigations have focused on *I. laurina* (Sw.) Willd. and *I. edulis* Mart. A complex triterpenoid saponin with immunological adjuvant activity has been reported in the leaves of *I. laurina* (Cruz et al., 2016). Galloyl depsides of tyrosine (Lokvam et al., 2007), flavonol glycosides (Martins et al., 2019), and proanthocyanidins (De Moura Martins et al., 2020) have also been reported from this species. Flavones, flavonol glycosides and phenolic acids have been identified in *I. edulis* (Correa, 1995; Lima et al., 2020; Tchuenmogne et al., 2013). Phytochemical information on other species is scarce. Flavonoids have been isolated from *I. fendleriana* Benth (Pistelli et al., 2009). and *I. alba* (Sw.) Willd. (Garcia et al., 2021), while cinnamoyl glucosides of catechin and

☆ In Memoriam of Prof. Mahabir Gupta, who tragically passed away during the preparation of this manuscript; with our profound gratitude for over 30 years of fruitful collaboration.

* Corresponding author.
E-mail address: olivier.potterat@unibas.ch (O. Potterat).

https://doi.org/10.1016/j.phytochem.2022.113183
Received 7 October 2021; Received in revised form 23 March 2022; Accepted 31 March 2022
Available online 7 April 2022

procyanidin dimers have been reported from *I. umbellifera* (Vahl) DC. (Lokvam et al., 2004). Recently, a derivative of menthiafolic acid was isolated from the trunk wood of *I. alba*. (Garcia et al., 2021).

Here we report on the isolation and characterization of constituents from the *I. sapindoides* leaf extract inhibiting *P. viticola*, which were found to be a series of acacic acid-type bidesmosidic saponins (Fig. 1).

2. Results and discussion

The activity in the MeOH extract was assigned by HPLC time-based fractionation, whereby the microfractions collected were tested for their antifungal activity against *P. viticola* zoospores. The activity profile correlated with a broad and poorly resolved peak eluting with 43–56% MeCN in the HPLC-UV trace (Fig S1, Supporting information). Noteworthy, the peak and the activity did not disappear when the extract was passed through a polyamide cartridge to remove possible tannins (data not shown).

For preparative isolation, a large batch of *I. sapindoides* leaves was extracted with 96% ethanol. The ethanolic extract (MIC_{100} 25 μg/mL) was successively partitioned between H_2O and *n*-hexane, ethyl acetate and *n*-butanol. The *n*-BuOH-soluble fraction (MIC_{100} 8 μg/mL) was shown to contain the peak previously detected in the active window of the chromatogram. This fraction was further separated by open column chromatography on silica gel, followed by preparative HPLC on a HILIC, and semi-preparative HPLC on a C_{18} column. Compounds **1**–**3** were obtained, in part as mixtures of *E/Z* isomers designated as **a** and **b**, respectively.

Compound **1a/b** had a molecular formula of $C_{97}H_{147}NO_{45}$ as determined by HRESIMS (*m/z* 2044.9186 $[M\text{-}H]^-$; calcd. for $C_{97}H_{146}NO_{45}^-$ 2044.9167). The ^1H and ^{13}C NMR spectra displayed resonances characteristic of an oleanane type triterpene. In the ^1H NMR spectrum, seven tertiary methyl signals at δ_H 0.63, 0.65, 0.77, 0.85, 0.89, 0.92, and 1.33, and an olefinic proton at δ_H 5.27 showed HSQC correlations to the corresponding carbons at δ_C 16.1 (C-24), 16.3 (C-26), 28.5 (C-30), 15.2 (C-25), 27.4 (C-23), 18.4 (C-29), 26.3 (C-27), and 121.8 (C-12), respectively. The presence of oxygen atoms at C-16 (δ_H 4.35, δ_C 72.1) and C-21 (δ_H 5.41, δ_C 75.8) was assigned by comparison with literature data (Liu et al., 2009) and was also supported for the latter by HMBC correlations from H_3C-29 and H_3C-30 to C-21. The relative configuration of the triterpenoid was established on the basis of NOESY correlations: on one face from H-3 to H-23 and H-5, H-5 to H-9, H-9 to H-27, H-27 to C-16-OH, C-16-OH to H-21, H-21 to H-30 and, on the other face, from H-24 to H-25, and from H-25 to H-26. On the basis of these data, the structure of the triterpenoidal aglycone was established as (3β, 16α, 21β)-3,16,21-trihydroxy-oleanolic acid, also known as acacic acid.

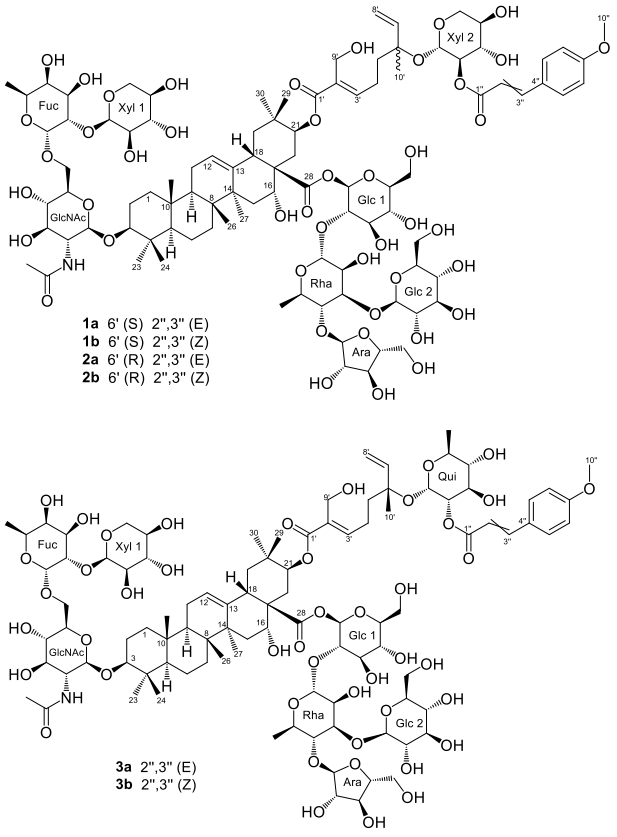

Fig. 1. Saponins isolated from *I. sapindoides*.

Acid hydrolysis yielded L-arabinose, D-fucose, D-glucose, D-glucosamine, L-rhamnose and D-xylose which were identified by GC analysis after derivatization with (+)-2-butanol-acetyl chloride. In the ^1H NMR spectrum of **1** anomeric proton signals were observed at δ_H 4.25 (d, J = 8.0 Hz, H-1 of GlcNAc), 4.36 (overlapped, H-1 of Fuc), 4.31 (d, J = 7.1 Hz, H-1 of Xyl 1), 4.46 d, J = 7.8 Hz, H-1 of Xyl 2 for **1a**) or 4.42 (d, J = 8.0 Hz, H-1 of Xyl 2 for **1b**), 5.23 (d, J = 7.6 Hz, H-1 of Glc 1), 4.35 (overlapped, H-1 of Glc 2), 5.02 (br s, H-1 of Rha), and 5.20 (br s, H-1 of Ara). They correlated with carbon resonances at δ_C 103.1 (C-1 of GlcNAc), 101.7 (C-1 of Fuc), 105.0 (C-1 of Xyl 1), 96.2 (C-1 of Xyl-2), 93.4 (C-1 of Glc 1), 103.6 (C-1 of Glc 2), 99.9 (C-1 of Rha), and 108.8 (C-1 of Ara) in the HSQC spectrum. The anomeric configuration of the sugar residues was established from the coupling constant of the anomeric protons, and from ^{13}C NMR data in the case of the rhamnosyl residue (similar dihedral angles in both anomers) and sugars with overlapped anomeric proton signal. The presence of a N-acetyl group (δ_H 1.76, δ_C 22.9, 166.8) on the glucosamine residue was supported by the HMBC correlation between H-2 (δ_H 3.39) of the glucosamine and the acetyl carbonyl (δ_C 168.6).

Additional resonances observed in the ^1H and ^{13}C NMR spectra were assigned to a monoterpenoid unit containing one ester carbonyl (δ_C 166.0, C-1′), two double bonds including an exocyclic methylene at δ_C 132.4 (C-2′), 144,2 (C-3′), 141.8 (C-7′) and 115.0 (C-8′), three *sp3* methylenes at δ_C 22.3 (C-4′), 39.6 (C-5′), and 54.5 (C-9′), a non-protonated *sp3* carbon at δ_C 78.7 (C-6′), and a tertiary methyl at δ_C 23.2 (C-10′). The full structure of the monoterpenoid was established as 6-hydroxy-2-(hydroxymethyl)-6-methyl-2,7-octadienoic acid with the aid of HMBC correlations and by comparison with literature data (Liu et al., 2009; Zou et al., 2005). The configuration at C-6′ was assigned as *S* by comparison of the ^{13}C NMR data with those reported for both configurations (Liu et al., 2009; Zheng et al., 2006; Zou et al., 2005, 2010). The HMBC correlation between H-21 (δ_H 5.41) and C-1' of the monoterpenoid residue (δ_C 166.0) indicated the position of attachment at the triterpenoid moiety.

Signals for a methoxy group (δ_H 3.78, δC 55.1), and resonances in the low field region were attributed to a *p*-methoxycinnamic acid residue. They included one ester carbonyl (δ_C 165.4, C-1″), two vinyl signals from a *E* double bond [δ_C 115.3 (C-2″), δ_H 6.47 (1H, d, J = 16.0 Hz, H-2″); δ_C 144.1 (C-3″), δ_H 7.60 (1H, d, J = 15.8, H-3″)], and aromatic signals from a *para*-substituted benzene ring [δ_C 126.5 (C-4″); δ_H 7.66 (2H, d, J = 8.5 Hz) δ_C 129.9, (H/C-5″, 9″); δ_H 6.96 (2H, d, J = 8.5 Hz), δ_C 114.2, (H/C-6″, 8''); δ_C 161.0 (C-7″)]. However, for the double bond a second set of signals was observed [δ_H 5.83 (1H, d, J = 12.8 Hz), δ_C 116.4 (H/C-2″); δ_H 7.61 (1H, d, overlapped, δ_C 116.4 (H/C-3″)] which indicated the presence of the *Z* isomer (**1b**) as additional compound. This was further confirmed by HPLC-DAD analysis of the isolated product which revealed the presence of two peaks with UV spectra corresponding to *E* and *Z* *p*-methoxycinnamoyl chromophores, respectively (Fig. S4). A HMBC correlation between H-2 of the xylose residue and C-1'' established the esterification position of the *p*-methoxycinnamic acid.

The HMBC correlations between H-1 of GlcNAc (δ_H 4.25) and C-3 of the aglycon (δ_C 87.3), and between H-1 of Glc I (δ_H 5.23) and C-28 of the aglycon (δ_C 172.8) indicated that the N-acetylglucosamine and a

glucosyl residue were attached to C-3 and C-28, respectively. The HMBC cross peak between H-1 of Xyl-2 and C-6' indicated the linkage of a xylose residue on the monoterpene moiety. The interglycosidic linkages were established from key HMBC and COSY correlations as shown in Fig. 2. The *α*-L-arabinofuranosyl-(1 → 4)-*O*-[*β*-D-glucopyranosyl-(1 → 3)]-*O*-*α*-L-rhamnopyranosyl-(1 → 2)-*O*-*β*-D-glucopyranosyl tetraglycosidic chain at C-28 is a typical structural feature in acacic acid-type saponins and is found, among others, in ingasaponin (Cruz et al., 2016) and julibrosides (Zheng et al., 2006). As to the glycosidic chain at C-3, the chemical shifts of H-2 of Fuc (δ_H 3.43) and H-3 of Fuc (δ_H 3.44) were too close to assign their position from COSY and HMBC correlations. The attachment of the xylose 1 residue at C-2 of the fucose was determined based on the comparison of the ^{13}C NMR chemical shifts with those reported for julibrosides J_{29} and J_{30} which possess the same glycosidic chain (Zheng et al., 2006). This was further supported by chemical shift calculations in DMSO-d_6 with ADC/Labs software (ACD/Labs, Toronto, Canada). The *β*-D-xylopyranosyl-(1 → 2)-*O*-*β*-D-fucopyranosyl-(1 → 6)-*N*-acetyl-*β*-D-glucosaminopyranosyl triglycosidic chain at C-3 is also found in several acacic acid-type saponins. The structure of compound **1**, named ingadoside A, is shown in Fig. 1.

Compound **2a/b** had the same molecular formula $C_{97}H_{147}NO_{45}$ as **1** (HRESIMS *m/z* 2044.9183 [M-H]$^-$; calcd. for $C_{97}H_{146}NO_{45}^-$ 2044.9167). Acid hydrolysis yielded identical monosaccharides. The ^{1}H and ^{13}C NMR data, including HMBC correlations, were highly similar to those of **1a/b**. However, slight differences were observed for the resonances of C-5′ (δ_C 38.2), and C-7′ (δ_C 142.5) of the monoterpenoid moiety, and were indicative of the *R* configuration at C-6′ (Liu et al., 2009; Zheng et al., 2006; Zou et al., 2005, 2010). Compound **2a/b** was thus the C-6′ epimer of **1a/b**. Similar to **1a/b,** compound **2**, named ingadoside B, was also obtained as a mixture of *E* (**2a**) and *Z* (**2b**) isomers (Fig. 1).

Compound **3a/b** had a molecular formula of $C_{98}H_{149}NO_{45}$, as deduced from the [M-H]$^-$ HRESIMS pseudomolecular ion at *m/z* 2058.9329 (calcd. for $C_{98}H_{148}NO_{45}^-$, 2058.9323). The ^{1}H and ^{13}C NMR signals of **3a/b** were comparable to those of compound **2a/b**, but suggested that a xylose residue was replaced by a D-quinovose. This was also supported by GC analysis after acid hydrolysis of **2**. A HMBC correlation between H-1 of the quinovose residue (δ_H 4.44, *d*, *J* = 7.9 Hz) and C-6' (δ_C 78.8) confirmed that a quinovose was attached to the monoterpene unit instead of a xylose as in **2a/b**. The *R* configuration of the monoterpene moiety was established from the ^{13}C NMR data in comparison with literature values (Liu et al., 2009; Zou et al., 2005). In contrast to compounds **1a/b** and **2a/b**, a sample of **3** could be obtained in pure *E* isomeric form (**3a**). This was possible due to particular precautions that were taken for the sample work-up after the final HPLC purification step. The structure of compound **3**, named ingadoside C, is shown on Fig. 1.

Photo-induced *E/Z* isomerization is common in cinnamic acid derivatives and has been widely reported (Caccamese et al., 1979; Kort et al., 1996). In the case of compounds **1a/b** and **2a/b**, a baseline separation of both isomers, identifiable by their distinctly different UV spectra, could be achieved by HPLC (Fig. S4). Evaporation of each sample, however, yielded again a mixture of both isomers. Given the limited amounts of compounds no further purification under strict exclusion of light was attempted. Compound **3a/b** was purified after **1a/b** and **2a/b**, and particular precautions were taken to strictly prevent exposure of the sample to light and heat after HPLC separation. By doing so, the *E* isomer (**3a**) could be obtained in pure form. However, the later eluting *Z* isomer was still mixed with minor amounts of the *E* isomer. In this case this was likely due to the non-baseline HPLC separation of the isomers rather than to an isomerization after isolation (Fig. S5).

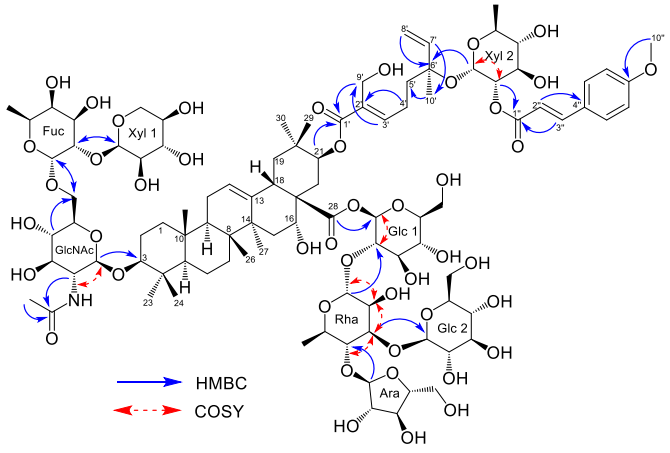

Fig. 2. Key HMBC and COSY correlations for compound **1a**.

The compounds and intermediate fractions were tested for their inhibitory effect on *P. viticola* zoospore formation and activity (Table 3). Saponins **1**–**3** showed potent activity, with MIC_{100} values of 3 or 6 μg/mL. Compounds **1** and **2** containing a xylose instead of a quinovose residue attached to the monoterpenoid showed slightly stronger activity. On the other hand, the configuration at C-6' had no effect on the potency. Interestingly, the crude saponin fractions F7.6 and F7.7 were equally active as the pure compounds. This suggests that additional saponins with comparable potency contribute to the activity.

Activity of the 96% ethanolic extract was further investigated on grapevine plantlets under controlled conditions in comparison with a copper reference treatment (Table 4). Compared to non-treated plants, the *I. sapindoides* ethanolic extract reduced grapevine downy mildew caused by *P. viticola* by 96% or 97% at 0.5 mg/mL in two independent experiments, and its efficacy was comparable to a standard copper treatment.

While this is the first report of saponins in *I. sapindoides*, compounds **1**–**3** share some structural features with ingasaponin, a compound that has been previously isolated from *I. laurina* (Cruz et al., 2016). Ingasaponin differs, however, by the presence of four monoterpenoid units and the absence of a cinnamoyl residue. Compounds **1**–**3** belong to a group of approx. 70 saponins bearing this particular monoterpenoid esterified at C-21 of acacic acid. They have been reported so far only in plants of the family Fabaceae, particularly in the genera *Albizia* (e.g. julibrosides) and *Acacia* (e.g. avicins) (Lacaille-Dubois et al., 2011). About half of these compounds also contain a N-acetylglucosamine residue attached at C-3, but in contrast to **1**–**3**, they all lack a cinnamoyl residue.

It is worth mentioning that several additional peaks with molecular weights in the same mass range and with similar UV spectra were detected during the isolation of saponins **1**–**3** (For a HPLC profile of the saponin fractions F7.6 and F7.7 see Supporting information, Fig S3). Even though we used a combination of different column chemistries and mobile phases, they could not be obtained in pure form. *I. sapindoides* appears therefore to contain a highly complex mixture of structurally similar saponins which probably all contribute to the antifungal activity.

Saponins with antifungal activity have been widely reported (De Moura Martins et al., 2020; Guo et al., 2018; Hu et al., 2018; Lanzotti et al., 2012; Liu et al., 2009; Wolters, 1966). The activity is attributed to the interaction with sterols present as essential membrane components in all eukaryotes, thereby leading to cell lysis (Zaynab et al., 2021). Against *P. viticola*, a very good efficacy under controlled conditions has been found for several plant protection products containing saponins (e.g. based on extracts from *Yucca schidigera* Roezl ex Ortgies or *Quillaja saponaria* Molina) (Dagostin et al., 2011). Yet, their efficacy under field conditions was only moderate, maybe due to limited rain fastness.

3. Conclusion

Polar extracts of *I. sapindoides* were identified as promising candidates for the development of new natural pesticides to replace or reduce the use of copper in organic agriculture. Targeted isolation of the active constituents resulted in the characterization of three acacic acid-type bidesmosidic saponins which strongly inhibit *P. viticola* zoospores. *I. sapindoides* is grown as a shading tree in coffee plantations. The plant

Table 1
^{1}H and ^{13}C NMR spectroscopic data of the aglycone, monoterpene and *p*-methoxycinnamic acid moieties of **1**–**3** in DMSO-d_6.

Position	1a/b		2a/b		3a/b	
	δ_C, type	δ_H (*J* in Hz)	δ_C, type	δ_H (*J* in Hz)	δ_C, type	δ_H (*J* in Hz)
1	37.8, CH_2	0.97	38.0, CH_2	0.97	38.0, CH_2	0.97
		1.49		1.49		1.49
2	25.3, CH_2	1.47	25.6, CH_2	1.47	25.5, CH_2	1.47
		1.79		1.79		1.79
3	87.3, CH	3.11	87.4, CH	3.11	87.4, CH	3.11
4	38.2, C		38.5, C		38.4, C	
5	54.9, CH	0.70	55.1, CH	0.69	55.0, CH	0.69
6	17.7, CH_2	1.25	17.9, CH_2	1.24	17.9, CH_2	1.25
		1.48		1.48		1.49
7	32.4, CH_2	1.31	32.6, CH_2	1.31	32.6, CH_2	1.31
		1.41		1.41		1.39
8	38.8, C		39.1, C		39.0, C	
9	45.8, CH	1.54	46.1, CH	1.55	46.0, CH	1.55
10	36.1, C		36.3, C		36.3, C	
11	22.7, CH_2	1.81	22.9, CH_2	1.81	22.9, CH_2	1.80
12	121.8, CH	5.27, m	122.1, CH	5.27, m	122.0, CH	5.28, m
13	142.0, C		142.2, C		142.1, C	
14	40.6, C		40.9, C		40.8, C	
15	34.3, CH_2	1.39	34.5, CH_2	1.39	34.5, CH_2	1.40
		1.47		1.47		1.48
16	72.1, CH	4.35	72.3, CH	4.35	72.2, CH	4.35
17	49.9, C		50.2, C		50.2, C	
18	39.6, CH	2.86, m	39.9, CH	2.86, m	39.8, CH	2.87, m
19	46.8, CH_2	1.13	47.0, CH_2	1.13	47.0, CH_2	1.15
		2.41, m		2.41, m		2.42, m
20	34.3, C		34.6, C		34.5, C	
21	75.8, CH	5.41, m	76.1, CH	5.42, m	76.0, CH	5.43, m
22	35.0, CH_2	1.47	35.3, CH_2	1.48	35.2, CH_2	1.48
		2.01, m		2.02, m		2.02, m
23	27.4, CH_3	0.89, s	27.6, CH_3	0.89, s	27.6, CH_3	0.89, s
24	16.1, CH_3	0.63, s	16.4, CH_3	0.63, s	16.3, CH_3	0.64, s
25	15.2, CH_3	0.85, s	15.4, CH_3	0.85, s	15.4, CH_3	0.85, s
26	16.3, CH_3	0.65, s	16.5, CH_3	0.65, s	16.5, CH_3	0.65, s
27	26.3, CH_3	1.33, s	26.5, CH_3	1.33, s	26.5, CH_3	1.34, s
28	172.8, C		173.1, C		172.9, C	
29	18.4, CH_3	0.92, s	18.7, CH_3	0.93, s	18.7, CH_3	0.94, s
30	28.5, CH_3	0.77, s	28.8, CH_3	0.78, s	28.7, CH_3	0.79, s
16-OH		4.85, br s		4.86, br s		4.87, br s
Monoterpene						
1′	166.0, C		166.3, C		166.2, C	
2′	132.4, C		132.6, C		132.5, C	
3′	144.2, CH	6.58, t (7.5)	144.5, CH	6.61, m	144.5, CH	6.63, t (7.3)
4′	22.3, CH_2	2.23, m	22.4, CH_2	2.18, m	22.4, CH_2	2.21, m
5′	39.6, CH_2	1.52	38.2, CH_2	1.57	37.6, CH_2	1.59
6′	78.7, C		78.9, C		78.8, C	
7′	141.8, CH	5.67, ddd (17.7, 10.8, 7.2)	142.5, CH	5.81	142.6, CH	5.80
8′	115.0, CH_2	5.16, m	114.8, CH_2	5.13, m	114.6, CH_2	5.12, m
9′	54.5, CH_2	4.04	54.8, CH_2	4.06	54.8, CH_2	4.07
10′	23.2, CH_3	1.23	23.4, CH_3	1.14	23.7, CH_3	1.13
***p*-methoxycinnamic acid**						
1′′ *E*	165.4, C		165.6, C		164.8, C	
1′′ *Z*	164.7, C		164.9, C		ND	
2′′ *E*	115.3, CH	6.47, d (16.0)	115.6, CH	6.46, d (16.0)	115.6, CH	6.46, d (16.0)
2′′ *Z*	116.4, CH	5.83, d (12.7)	116.7, CH	5.83	116.6, CH	5.83
3′′ *E*	144.1, CH	7.60, d (15.8)	144.3, CH	7.61, d (15.8)	144.5, CH	7.61, d (15.9)
3′′ *Z*	142.6, CH	6.93	142.7, CH	6.90	142.6, CH	6.90
4′′ *E*	126.5, C		126.7, C		126.8, C	
4′′ *Z*	126.7, C		126.9, C		ND	
5′′ *E*	129.9, CH	7.66, br d (8.7)	130.2, CH	7.66, br d (8.9)	130.1, CH	7.66, br d (8.9)
5′′ *Z*	132.4, CH	7.73, br d (8.7)	132.4, CH	7.75, br d (8.9)	132.4, CH	7.75, br d (8.5)
6′′ *E*	114.2, CH	6.97, d (8.9)	114.5, CH	6.96, d (8.7)	114.4, CH	6.96, d (8.5)
6′′ *Z*	113.2, CH	6.89	113.5, CH	6.91	113.4, CH	6.91
7′′ *E*	161.0, C		161.2, C		160.1, C	
7′′ *Z*	160.0, C		160.2, C		ND	
8′′ *E*	114.2, CH	6.97, d (8.9)	114.5, CH	6.96, d (8.7)	114.4, CH	6.96, d (8.5)
8′′ *Z*	113.2, CH	6.89	113.5, CH	6.91	113.4, CH	6.91
9′′ *E*	129.9, CH	7.66, br d (8.7)	130.2, CH	7.66, br d (8.9)	130.1, CH	7.66, br d (8.9)
9′′ *Z*	132.4, CH	7.74, br d (8.7)	132.4, CH	7.75, br d (8.9)	132.4, CH	7.75, br d (8.5)
10′′ *E*	55.1, CH_3	3.78, s	55.4, CH_3	3.80, s	55.3, CH_3	3.79, s
10′′ *Z*	55.0, CH_3	3.77, s	55.2, CH_3	3.77, s	55.2, CH_3	3.77, s

Compounds **1a/b** and **2a/b** at 600 MHz for ^{1}H and 151 MHz for ^{13}C NMR.
Compound **3a/b** at 500 MHz for ^{1}H and 126 MHz for ^{13}C NMR.
Overlapped signals are reported without multiplicity.
ND: signal not detected due to amount of compound.
Assignments are based on COSY, ROESY, HSQC, HSQC-TOCSY, and HMBC spectra.

Table 2
^{1}H and ^{13}C NMR spectroscopic data of the glycosidic moiety of **1**–**3** in DMSO-d_6.

Position	1a/b		2a/b		3a/b	
	δ_C, type	δ_H (J in Hz)	δ_C, type	δ_H (J in Hz)	δ_C, type	δ_H (J in Hz)
Sugar moiety C-3						
GlcNAc						
1	103.1, CH	4.25, d (8.0)	103.3, CH	4.25, d (8.2)	103.3, CH	4.25, d (8.2)
2	55.5, CH	3.39	55.8, CH	3.39	55.7, CH	3.39
3	73.7, CH	3.26	74.0, CH	3.26	73.9, CH	3.26
4	70.6, CH	3.0, t (8.8)	70.9, CH	3.00, t (9.3)	70.8, CH	2.99, t (9.0)
5	75.5, CH	3.27	75.7, CH	3.27	75.7, CH	3.27
6	68.1, CH_2	3.55 3.89, d (10.7)	68.4, CH_2	3.55 3.89, d (10.7)	68.4, CH_2	3.54 3.89, d (11.0)
7	168.6, C		168.8, C		168.6, C	
8	22.9, CH_3	1.76, s	23.2, CH_3	1.76, s	23.2, CH_3	1.76, s
Fuc						
1	101.7, CH	4.36	101.9, CH	4.37	101.9, CH	4.37
2	80.2, CH	3.43	80.4, CH	3.44	80.3, CH	3.44
3	73.1, CH	3.44	73.4, CH	3.44	73.3, CH	3.45
4	70.3, CH	3.44	70.5, CH	3.44	70.4, CH	3.44
5	69.6, CH	3.47	69.8, CH	3.47	69.8, CH	3.47
6	16.4, CH_3	1.13	16.6, CH_3	1.12	16.6, CH_3	1.13
Xyl 1						
1	105.0, CH	4.31, d (7.1)	105.2, CH	4.31, d (7.3)	105.2, CH	4.31, d (7.3)
2	74.3, CH	3.06	74.5, CH	3.06	74.5, CH	3.06
3	75.6, CH	3.15	75.8, CH	3.15	75.8, CH	3.15
4	69.3, CH	3.28	69.5, CH	3.29	69.5, CH	3.28
5	65.5, CH_2	3.08 3.78	65.7, CH_2	3.07 3.78	65.7, CH_2	3.07 3.78
Sugar moiety at C-28						
Glc 1						
1	93.4, CH	5.23, d (7.6)	93.6, CH	5.24, d (7.6)	93.6, CH	5.24, d (7.6)
2	75.3, CH	3.30	75.5, CH	3.30	75.5, CH	3.30
3	76.5, CH	3.36	76.7, CH	3.36	76.7, CH	3.36
4	69.5, CH	3.14	69.7, CH	3.14	69.6, CH	3.15
5	77.4, CH	3.17	77.6, CH	3.16	77.5, CH	3.18
6	60.2, CH_2	3.42 3.58	60.5, CH_2	3.42 3.57	60.4, CH_2	3.42 3.57
Glc 2						
1	103.6, CH	4.35	103.9, CH	4.35	103.8, CH	4.36
2	73.6, CH	3.06	73.8, CH	3.05	73.8, CH	3.06
3	76.5, CH	3.14	76.8, CH	3.14	76.7, CH	3.14
4	69.6, CH	3.12	69.9, CH	3.12	69.8, CH	3.12
5	76.1, CH	3.12	76.4, CH	3.12	76.3, CH	3.12
6	60.6, CH_2	3.47 3.63	60.9, CH_2	3.47 3.63	60.8, CH_2	3.48 3.64
Rha						
1		5.02, br s		5.02, br s		5.02, br s
2	68.8, CH	4.05	69.0, CH	4.04	68.9, CH	4.05
3	79.9, CH	3.76	80.1, CH	3.76	80.1, CH	3.77
4	76.4, CH	3.47	76.6, CH	3.47	76.5, CH	3.47
5	67.2, CH	3.64	67.4, CH	3.64	67.4, CH	3.64
6	17.7, CH_3	1.17	17.9, CH_3	1.17	17.9, CH_3	1.17
Ara						
1	108.8, CH	5.20, br s	109.0, CH	5.21, br s	109.0, CH	5.20, br s
2	82.3, CH	3.86, br s	82.6, CH	3.86, br s	82.5, CH	3.86, br s
3	76.8, CH	3.65	77.0, CH	3.66	77.0, CH	3.66
4	83.7, CH	3.79	84.0, CH	3.79	83.9, CH	3.79
5	61.1, CH_2	3.47 3.53	61.3, CH_2	3.43 3.53	61.3, CH_2	3.43 3.54
Sugar moiety at C-6′						
Xyl 2/ Qui	**Xyl 2**		**Xyl 2**		**Qui**	
1 *E*	96.2, CH	4.46, d (7.8)	96.3, CH	4.44, d (8.0)	95.2, CH	4.44, d (8.2)
1 *Z*	96.0, CH	4.42, d (8.0)	96.2, CH	4.40, d (8.0)	95.3, CH	4.40
2 *E*	73.5, CH	4.63, t (8.9)	73.8, CH	4.62	ND	ND
2 *Z*	73.4, CH	4.60	73.6, CH	4.58, t (8.7)	73.8, CH	4.60
3	74.1, CH	3.35	74.3, CH	3.36	73.9, CH	3.35
4	69.4, CH	3.17	69.6, CH	3.15	75.5, CH	2.90
5	65.4, CH_2	3.11 3.68	65.8, CH_2	3.09 3.78	71.4, CH	3.20
6					17.9, CH_3	1.14

Compound **3a**/**b** at 500 MHz for ^{1}H and 126 MHz for ^{13}C NMR.
Compounds **1a**/**b** and **2a**/**b** at 600 MHz for ^{1}H and 151 MHz for ^{13}C NMR.
Overlapped signals are reported without multiplicity.
ND: signal not detected due to amount of compound.
Assignments are based on COSY, ROESY, HSQC, HSQC-TOCSY and HMBC spectra.

Table 3
In vitro Minimal Inhibitory Concentrations (MIC_{100}) of *I. sapindoides* extract, fractions and isolated compounds against *Plasmopara viticola*.

Sample	MIC_{100} [µg/mL][a]
96% EtOH extract	25
n-BuOH soluble fraction	8
Fr. F7	5
Fr. F7.6	3
Fr. F7.7	3
1a/**b**[b]	6
2a/**b**[b]	6
3a/**b**[b]	3

[a] MIC values are reported as mean of 4 independent replicates.
[b] Tested as *E*/*Z* isomeric mixtures.

may therefore provide a sustainable source for the production of extracts to be used as natural pesticides. As a next step, appropriate formulations should be designed to ensure stability and rain fastness of the product.

Table 4
Plant disease reduction by treatment with 96% EtOH *I. sapindoides* extract and Cu reference.

Treatment	Concentration (mg/mL)	Experiment 1			Experiment 2		
		Infected leaf area (%)		Efficacy (%)[c]	Infected leaf area (%)		Efficacy (%)
		Mean	SD		Mean	SD	
Control		71	12		82	11	
Cu reference[a]	0.3[b]	0	0	100	0	0	100
I. sapindoides extract[d]	1	2	3	97	3	8	96
	0.5	3	2	96	2	3	97
	0.25	11	9	84	29	11	64

[a] Cu in the form of $Cu(OH)_2$ (Kocide® Opti, Bayer, AG).
[b] Concentration of Cu^{2+} ions.
[c] Percentage disease reduction compared to untreated control.
[d] Experiment 1: Small-scale ethanolic extract dissolved in DMSO; Experiment 2: Herbamed-extract formulated as a wettable powder.

4. Experimental

4.1. General experimental procedures

Ultrapure water was obtained from a Milli-Q water purification system (Merck Millipore, Darmstadt, Germany). HPLC-grade acetonitrile, chloroform and methanol were purchased from Avantor Performance Materials (Radnor Township, PA, USA). HPLC-grade *n*-butanol, ethyl acetate, and formic acid were obtained from Scharlau (Scharlab S. L., Spain). Technical grade ethyl acetate and *n*-hexane were from Scharlau and were redistilled before use. Acetyl chloride, (*S*)-(+)-2-butanol, and trifluoroacetic anhydride (TFAA) were bought from TCI Chemicals (Japan). L-Arabinose, D-fucose, D-glucose, D-quinovose, L-rhamnose, D-xylose (all Sigma-Aldrich, St.-Louis, MI, USA), and D-glucosamine (Biosynth Carbosynth, Thal, Switzerland) were used as reference monosaccharides for sugar analysis. Vanillin was obtained from Roth (Carl Roth GmbH + Co, Karlsruhe, Germany). Silica gel 60 F254 coated aluminum TLC plates, and silica gel (0.043–0.063 mm) for open-column chromatography were obtained from Merck KGaA (Darmstadt, Germany). TLC plates were visualized under UV light and by spraying with 1% vanillin in EtOH and 10% sulfuric acid in EtOH, followed by heating at 110 °C.

HPLC-PDA-ELSD-ESIMS analyses were performed on system consisting of a degasser, a quaternary pump (LC-20AD), a column oven (CTO-20AC), a PDA detector (SPD-M20A), a triple quadrupole mass spectrometer (LCMS-8030) (all Shimadzu, Kyoto, Japan), and an ELSD 3300 detector (Alltech Associates, Deerfield, IL, USA). Separations were performed on a SunFire C_{18} (3.5 μm, 150 × 3.0 mm i.d.) column equipped with a guard column (10 mm × 3.0 mm i.d.) (Waters, Milford, MA, USA), a NUCLEODUR HILIC column (5 μm, 3.0 × 150 mm i.d., Macherey-Nagel, Düren, Germany), or a ReproSil-Pur 120 C18-AQ column (3 μm, 3.0 × 150 mm i.d., Dr. Maisch, Ammerbuch, Germany). LabSolutions software (Shimadzu) was used for data acquisition and processing.

Preparative HPLC was carried out on a Preparative LC/MSD System (Agilent Technologies, Santa Clara, CA, USA) consisting of a binary pump (1260 Prep Bin Pump, 1290 Infinity II), a quaternary pump (G1311A Quat Pump, 1200 Series), a 1290 Infinity II Valve Drive manual injection system, a PDA detector (1100 Series), and a Quadrupole LC/MS (6120). A Nucleodur HILIC column (5 μm, 32 × 150 mm i.d., Macherey-Nagel), equipped with a Nucleodur HILIC guard column (10 × 32 mm i.d.), was used. The mobile phase consisted of 60% aq. MeOH (A) and MeCN (B) both containing 0.1% formic acid. An isocratic flow of 60% B at a flow rate of 20 mL/min was used. Detection wavelength was set to 300 nm. Data acquisition and processing was performed using ChemStation software (Agilent Technologies).

Semi-preparative HPLC separations were performed on an HP 1100 Series system (Agilent Technologies) consisting of a binary pump (G1312A BinPump), an autosampler (G1367A WPALS), a column oven (G1316A COLCOM), and a diode array detector (G1315A DAD). A ReproSil-Pur 120 C18-AQ column (3 μm, 10 × 150 mm i.d., Dr. Maisch, Germany) was used, if not otherwise stated. The flow rate was 4 mL/min, and the detection wavelength was set at 300 nm. Data acquisition and processing was performed using ChemStation software (Agilent Technologies).

NMR spectroscopic data of **1a**/**b** and **2a**/**b** were obtained on a Bruker Avance Neo 600 MHz NMR spectrometer operating at 600 MHz for ^{1}H and 151 MHz for ^{13}C, and equipped with a QCI 5 mm Cryoprobe and a SampleJet automated sample changer (all Bruker, Rheinstetten, Germany). NMR spectra of compound **3a**/**b** were recorded on a Bruker Avance III spectrometer (Bruker, Fällanden, Switzerland) operating at 500 MHz for ^{1}H and 126 MHz for ^{13}C, and equipped with a 5 mm BBO probe at 23 °C. Spectra were measured in DMSO-d_6 (ARMAR Chemicals, Döttingen, Switzerland). Chemical shifts are reported in parts per million (δ) using the solvent signal (δ_H 2.50; δ_C 39.51) as internal reference; coupling constants (J) are given in Hz. Data were analyzed using Topspin (Bruker) and Spectrus Processor (ACD/Lab, Toronto, Canada) softwares. Optical rotation was measured on a JASCO P-2000 polarimeter (Brechbühler AG, Switzerland) equipped with a 10 cm temperature-controlled microcell.

HRESIMS data were recorded in negative ion mode on an Agilent 1290 Infinity system consisting of a binary pump (G4220A), autosampler (G4226A), column compartment (G1316C) and a 6540 UHD Accurate-Mass quadrupole time-of-flight detector (G6540A) (Agilent Technologies).

GCMS was performed on a Hewlett-Packard GC/MS system (G1503A) equipped with a mass selective detector (HP5973) and an ionization gauge controller (59864B) (Agilent Technologies). A J&W DM-225 GC column (30 m; i.d.: 0.25 mm; film thickness; 0.25 μm; Agilent Technologies) was used. Injector temperature was 280 °C. Helium (0.7 mL/min) was used as a carrier gas. Transfer line temperature was 240 °C. The following temperature program was applied: 60 °C hold for 1 min, increase to 240 °C at 10 °C/min followed by 5 min at 240 °C. EI ionization was in positive ion mode (electron energy: 2040 V; Full Scan: *m/z*: 50–700). Data acquisition was performed by MSD ChemStation D.03 software (Agilent Technologies), and data were processed with Spectrus Processor (ACD/Lab).

4.2. Plant material

Leaves of *Inga sapindoides* Willd. (Fabaceae) used for the preparation of the extract library sample and the HPLC-based activity profiling were collected in El Copé, Coclé Province, Panama in April 2007 by CIFLORPAN (Center for Pharmacognostic Research on Panamanian Flora), collection number CIFLORPAN 7033. Leaves used for the preparation of the extract used in the first experiment on grapevine seedlings were collected in Parque Nacional Soberania, Camino de Cruces, Panama in February 2003 by CIFLOPRPAN, collection number CIFLORPAN 5677. Leaves used for preparative isolation and the second experiment on grapevine seedlings were collected by CIFLORPAN in El Copé, Coclé

Province on January 26 and February 10, 2017, collection numbers FLORPAN 8868 and 8869. Voucher specimens have been deposited at the Herbarium of the University of Panama. The taxonomic identity was confirmed by Alex Espinosa, botanist at CIFLORPAN. The material was air-dried in Panama and transferred to University of Basel in March 2017. Voucher specimens (no. 980, 1012 and 1014) are also kept at the Division of Pharmaceutical Biology, Department of Pharmaceutical Sciences, University of Basel.

4.3. HPLC microfractionation for activity profiling

Microfractionation was performed by semi-preparative HPLC on a SunFire™ Prep C_{18} column (5 µm, 150 × 10 mm i.d., Waters) equipped with a guard column (10 × 10 mm i.d.). The mobile phase consisted of water with 0.1% formic acid (Solvent A) and acetonitrile containing 0.1% formic acid (Solvent B). A gradient of 5–100% B in 30 min was used, followed by isocratic conditions of 100% B for 5 min. The flow rate was 4.0 mL/min. The extract was dissolved in DMSO at a concentration of 25 mg/mL, centrifuged, and filtered. Two injections of 400 µL were performed (20 mg of extract in total). Microfractions were collected every 90 s from 2 to 35 min (22 fractions per injection). After removal of the eluent in a Genevac EZ-2 evaporator (SP Industries, Ipswich UK), the fractions were re-dissolved in 300 µL of methanol. The corresponding fractions obtained from the two separations were combined in a 96 deep well plate and dried. Micro-fractions were re-dissolved in 200 µL DMSO. Aliquots of 5.5 µL of each fraction were added to 104.5 µL of 'Evian' water ('concentration 1') and then diluted 1:10 (11 µL 'concentration 1' added to 99 µL 'Evian' water, 'concentration 2') and 1:100 (11 µL 'concentration 2' added to 99 µL 'Evian' water, then discarding 11 µL, 'concentration 3') in the test plate. For testing, 20 µL of a sporangia solution was added to the 99 µL test solution in each well. Activity was assessed after 2–3 h using a binocular (50 and 100 fold magnification).

4.4. Extraction and isolation

The MeOH extract used for HPLC-based activity profiling was obtained by successive extraction of dried powdered leaves with petroleum ether, EtOAc and MeOH using an ASE 200 Accelerated Solvent Extractor (Dionex Corporation, Sunnyvale, CA, USA). For each solvent, a total of three cycles were performed with the temperature set at 70 °C, and the pressure at 120 bar resulting in 6.0% (w/w) of MeOH extract. The extract used in the first experiment on grapevine seedlings was prepared by maceration of dried powdered leaves (20 g) with 96% EtOH (yield 5.4%). Large scale extraction of the leaves was performed at Herbamed AG, Bühler, Switzerland. 20 kg of dried powdered leaves were extracted by percolation with 200 kg of 96% (v/v) ethanol. The extract was concentrated by distillation to yield a viscous residue (5.44 kg, dry residue 27.4%). A portion of the residue (170 g) was resuspended in water (2.0 L) and successively partitioned with *n*-hexane (3 × 1.5 L), EtOAc (4 × 1.5 L), and *n*-BuOH (4 × 1.5 L) to yield 26.2 g, 46.6 g, 36.0 g and 58.8 g of dry *n*-hexane, EtOAc, *n*-BuOH and H_2O soluble fractions, respectively.

The *n*-BuOH soluble fraction was separated by open column chromatography on silica gel (400 × 11 mm i.d.) with EtOAc-MeOH-H_2O (14:3:3) as mobile phase. A total of 55 fractions were collected, which were combined based on TLC analysis ($CHCl_3$–MeOH–H_2O (65:35:5)) into 10 fractions (F1– F10). F7 (2 g) was further purified by preparative HILIC-HPLC with a mixture of 60% aq. MeOH and MeCN as mobile phase, (see 4.2) to afford 7 subfractions (F7.1 – F7.7). Separation of F.7.7 (70 mg) by semi-preparative RP-18 HPLC with MeCN-water (33:77, both containing 0.1% formic acid) afforded four peaks (t_R = 17.1 min, 6.2 mg; t_R = 18.2 min, 7.3 mg; t_R = 20.8 min, 3.0 mg; t_R = 22.3 min, 3.8 mg). After evaporation of the solvent, the two former peaks were found to be mixtures of **1a** and **1b**, while the latter peaks gave mixtures of **2a** and **2b**. Final purification of F7.6 (100 mg) with the same chromatographic system yielded compound **3a** (t_R = 17.5 min, 8.7 mg) and a second peak (t_R = 18.3 min, 6.7 mg) which, after drying, afforded a mixture of **3a** and **3b**.

4.4.1. (E/Z)-ingadoside A (1a/b)

White amorphous powder; $[\alpha]_D^{25}$ -18 (*c* 0.1, MeOH); ^{1}H NMR (600 MHz, DMSO-d_6) and ^{13}C NMR (151 MHz, DMSO- d_6), see Tables 1 and 2; HRESIMS *m/z* 2044.9186 $[M-H]^-$ (calcd. for $C_{97}H_{146}NO_{45}^-$ 2044.9167).

4.4.2. (E/Z)-ingadoside B (2a/b)

White amorphous powder; $[\alpha]_D^{25}$ -17 (*c* 0.1, MeOH); ^{1}H NMR (600 MHz, DMSO-d_6) and ^{13}C NMR (151 MHz, DMSO- d_6), see Tables 1 and 2; HRESIMS *m/z* 2044.9183 $[M-H]^-$ (calcd. for $C_{97}H_{146}NO_{45}^-$ 2044.9167).

4.4.3. (E/Z)-ingadoside C (3a/b)

White amorphous powder; $[\alpha]_D^{25}$ -19 (*c* 0.1, MeOH); ^{1}H NMR (500 MHz, DMSO-d_6) and ^{13}C NMR (125 MHz, DMSO-d_6), see Tables 1 and 2; HRESIMS *m/z* 2058.9329 $[M-H]^-$ (calcd. for $C_{98}H_{148}NO_{45}^-$ 2058.9323).

4.4.4. (E)-Ingadoside B (3a)

White amorphous powder; $[\alpha]_D^{25}$ -26 (*c* 0.1, MeOH); HRESIMS *m/z* 2058.9347 $[M-H]^-$ (calcd. for $C_{98}H_{148}NO_{45}^-$ 2058.9323).

4.5. Acid hydrolysis and sugar analysis

The compounds (1 mg) were separately hydrolyzed with 2 M HCl (1 mL) for 15 h at 100 °C. After cooling, the solution was extracted with ethyl acetate (2 × 1 mL). The aqueous phase was dried under reduced pressure and then treated with a mixture of (+)-2-butanol-acetyl chloride (10:0.5 (v/v); 1 mL) at 55 °C for 15 h. The mixture was dried under N_2, and the residue derivatized with TFAA-EtOAc (3:4 (v/v), 1 mL) at 55 °C for 10 min (Nuevo et al., 2018). Each sample (1 µL) was manually injected in split mode (1:10) into the gas chromatograph. Reference sugars L-arabinose, D-fucose, L-rhamnose, D-quinovose, D-xylose, D-glucose and D-glucosamine (1 mg each) were derivatized in the same manner.

4.6. In vitro Plasmopara viticola inhibition assay

Bioassays were conducted using a previously published protocol (Thuerig et al., 2016). *Plasmopara viticola* (Berk. & M.A. Curtis) Berl. & De Toni was maintained on grapevine (*Vitis vinifera* L.) seedlings 'Chasselas' by weekly reinoculation. *P. viticola* sporangia suspensions were prepared from previously infected plants by washing freshly sporulating grapevine leaves with water and filtering through cheese cloth.

Samples were dissolved in DMSO (10 mg/mL for extracts and fractions, or 5 mg/mL for pure compounds) and serially diluted in water in 96 well plates before adding sporangial suspension (20 µL, approx. 200′000 sporangia/mL), resulting in a final volume of 120 µL per well. Final concentrations of serial dilutions ranged from 100 to 0.1 ppm for extracts and fractions, while serial dilutions from 50 ppm to 0.05 ppm were used for pure compounds. DMSO alone was tested as negative control in at least two replicates in all relevant concentrations. The release and activity of zoospores was assessed 2–3 h after setup of the experiment. MIC_{100} values correspond to the concentration needed to completely inhibit the release and/or the activity of zoospores. The experiment was repeated four times with independent serial dilutions.

4.7. In vivo Plasmopara viticola assay

Plant pathogen bioassays were performed on grapevine seedlings cv. "Chasselas" grown in the greenhouse as described before (Thuerig et al., 2016). In short, plants were treated with the product when they had 3-4 fully grown leaves. Leaves were left to dry before inoculation with *P. viticola* (50′000 sp/mL). After inoculation, plants were kept at 80–99% relative humidity (RH) (20–21 °C) for 1 d. Then, plants were

grown at 60–80% RH and 20 °C for 5 d, before increasing humidity again to 80–99% RH to induce sporulation for disease assessment. The percentage area covered by sporulating lesions (disease severity) was visually assessed for each leaf and a mean calculated for each plant. Each experiment included a non-treated control and a copper reference (copper hydroxide, Kocide® Opti, DuPont, Wilmington, DE, USA) at a standard concentration (0.3 mg/mL copper ions) as used in practice. Dried *I. sapindoides* extracts were either dissolved in DMSO at 100 mg/mL (small scale EtOH extract), or formulated as a wettable powder to improve solubility and applicability [20% extract (Herbamed extract), 20% solvent, 51% carrier, 6% defoaming agent, 3% surfactant] before adding to water to give extract concentrations of 1, 0.5, and 0.25 mg/mL Each treatment consisted of six replicate plants. Percentage efficacy of the test products was calculated as (1-(mean disease severity in plants treated with product/mean disease severity in non-treated control))*100 for each test product.

Declaration of competing interest

The authors declare that they have no known competing financial interests or personal relationships that could have appeared to influence the work reported in this paper.

Acknowledgments

Thanks are due to Orlando Fertig (Division of Pharmaceutical Biology, University of Basel) for the sugar analysis, to Dr. Aitor Moreno (Bruker Biospin) for recording the NMR spectra of **1a/b** and **2a/b,** and to Timm Hettich (University of Applied Sciences Northwestern Switzerland) for measuring the HRESIMS data. FiBL thanks the Coop Sustainability Fund and the Federal Office for Agriculture for funding.

Appendix A. Supplementary data

Supplementary data to this article can be found online at https://doi.org/10.1016/j.phytochem.2022.113183.

References

Caccamese, S., Azzolina, R., Davino, M., 1979. Separation of cis and trans isomers of naturally occurring hydroxycinnamic acids by high-pressure liquid chromatography. Chromatographia 12, 545–547. https://doi.org/10.1007/BF02265471.

Correa, S.M.V., 1995. Constituents of roots of *Inga edulis* var. *parviflora*. Fitoter. Riv. di Stud. ed Appl. delle piante Med. = J. Study Med. Plants 66, 379.

Cruz, M.D.F.S.J., Pereira, G.M., Ribeiro, M.G., Da Silva, A.M., Tinoco, L.W., Da Silva, B. P., Parente, J.P., 2016. Ingasaponin, a complex triterpenoid saponin with immunological adjuvant activity from *Inga laurina*. Carbohydr. Res. 420, 23–31. https://doi.org/10.1016/j.carres.2015.11.008.

Dagostin, S., Schärer, H.J., Pertot, I., Tamm, L., 2011. Are there alternatives to copper for controlling grapevine downy mildew in organic viticulture? Crop Protect. 30, 776–788. https://doi.org/10.1016/j.cropro.2011.02.031.

De Moura Martins, C., Morais, S.A.L.d., Martins, M.M., Cunha, L.C.S., da Silva, V., C, Teixeira, T.L., Santiago, B., M, de Aquino, F.J.T., Nascimento, E.A., Chang, R., Martins, C.H.G., de Oliveira, A., 2020. Antifungal and cytotoxicity activities and new proanthocyanidins isolated from the barks of *Inga laurina* (Sw.) Willd. Phytochem. Lett. 40, 109–120. https://doi.org/10.1016/j.phytol.2020.10.001.

Garcia, M.G., Gomes, R.F., Nascimento, C.C., Oliveira, L.M., Thomasi, S.S., Ferreira, A.G., Lima, M.P., 2021. Isolation of new compounds from *Andira parviflora* and *Inga alba* wood residues using LC-DAD-SPE/NMR. Chem. Nat. Compd. 57, 300–305. https://doi.org/10.1007/s10600-021-03352-8.

Guo, N., Tong, T., Ren, N., Tu, Y., Li, B., 2018. Saponins from seeds of genus *Camellia*: phytochemistry and bioactivity. Phytochemistry 149, 42–55. https://doi.org/10.1016/j.phytochem.2018.02.002.

Hu, Q., Chen, Y.Y., Jiao, Q.Y., Khan, A., Li, F., Han, D.F., Cao, G.D., Lou, H.X., 2018. Triterpenoid saponins from the pulp of *Sapindus mukorossi* and their antifungal activities. Phytochemistry 147, 1–8. https://doi.org/10.1016/j.phytochem.2017.12.004.

Kort, R., Vonk, H., Xu, X., Hoff, W.D., Crielaard, W., Hellingwerf, K.J., 1996. Evidence for trans-cis isomerization of the *p*-coumaric acid chromophore as the photochemical basis of the photocycle of photoactive yellow protein. FEBS Lett. 382, 73–78. https://doi.org/10.1016/0014-5793(96)00149-4.

Küpper, H., Gotz, B., Mijovilovich, A., Küpper, F.C., Meyer-Klaucke, W., 2009. Complexation and toxicity of copper in higher plants. I. Characterization of copper accumulation, speciation, and toxicity in *Crassula helmsii* as a new copper accumulator. Plant Physiol. 151, 702–714. https://doi.org/10.1104/pp.109.139717.

Lacaille-Dubois, M.A., Pegnyemb, D.E., Noté, O.P., Mitaine-Offer, A.C., 2011. A review of acacic acid-type saponins from Leguminosae-Mimosoideae as potent cytotoxic and apoptosis inducing agents. Phytochemistry Rev. 10, 565–584. https://doi.org/10.1007/s11101-011-9218-0.

Lamichhane, J.R., Osdaghi, E., Behlau, F., Köhl, J., Jones, J.B., Aubertot, J.-N., 2018. Thirteen decades of antimicrobial copper compounds applied in agriculture. A review. Agron. Sustain. Dev. 38, 28. https://doi.org/10.1007/s13593-018-0503-9.

Lanzotti, V., Romano, A., Lanzuise, S., Bonanomi, G., Scala, F., 2012. Antifungal saponins from bulbs of white onion, *Allium cepa* L. Phytochemistry 74, 133–139. https://doi.org/10.1016/j.phytochem.2011.11.008.

Lima, N.M., Andrade, T.J.A.S., Silva, D.H.S., 2020. Dereplication of terpenes and phenolic compounds from *Inga edulis* extracts using HPLC-SPE-TT, RP-HPLC-PDA and NMR spectroscopy. Nat. Prod. Res. 1–5. https://doi.org/10.1080/14786419.2020.1786824, 0.

Liu, R., Ma, S., Yu, S., Pei, Y., Zhang, S., Chen, X., Zhang, J., 2009. Cytotoxic oleanane triterpene saponins from *Albizia chinensis*. J. Nat. Prod. 72, 632–639. https://doi.org/10.1021/np800576s.

Lokvam, J., Clausen, T.P., Grapov, D., Coley, P.D., Kursar, T.A., 2007. Galloyl depsides of tyrosine from young leaves of *Inga laurina*. J. Nat. Prod. 70, 134–136. https://doi.org/10.1021/np060491m.

Lokvam, J., Coley, P.D., Kursar, T.A., 2004. Cinnamoyl glucosides of catechin and dimeric procyanidins from young leaves of *Inga umbellifera* (Fabaceae). Phytochemistry 65, 351–358. https://doi.org/10.1016/j.phytochem.2003.11.012.

Martins, C.D.M., De Morais, S.A.L., Martins, M.M., Cunha, L.C.S., Da Silva, C.V., Martins, C.H.G., Leandro, L.F., De Oliveira, A., De Aquino, F.J.T., Do Nascimento, E. A., Chang, R., 2019. Chemical composition, antifungal, and cytotoxicity activities of *Inga laurina* (Sw.) Willd Leaves. Sci. World J. https://doi.org/10.1155/2019/9423658.

Napoli, M., Cecchi, S., Grassi, C., Baldi, A., Zanchi, C.A., Orlandini, S., 2019. Phytoextraction of copper from a contaminated soil using arable and vegetable crops. Chemosphere 219, 122–129. https://doi.org/10.1016/j.chemosphere.2018.12.017.

Nuevo, M., Cooper, G., Sandford, S.A., 2018. Deoxyribose and deoxysugar derivatives from photoprocessed astrophysical ice analogues and comparison to meteorites. Nat. Commun. 9, 5276. https://doi.org/10.1038/s41467-018-07693-x.

Pistelli, L., Bertoli, A., Noccioli, C., Mendez, J., Musmanno, R.A., Di Maggio, T., Coratza, G., 2009. Antimicrobial activity of *Inga fendleriana* extracts and isolated flavonoids. Nat. Prod. Commun. 4, 1679–1683. https://doi.org/10.1177/1934578x0900401214.

Street, G., 1980. Microbiology and pollution: the biodegradation of natural and synthetic organic compounds. Philos. Trans. R. Soc. Lond. B Biol. Sci. 290, 355–367. https://doi.org/10.1098/rstb.1980.0100.

Tchuenmogne, A.M.T., Donfack, E.V., Kongue, M.D.T., Lenta, B.N., Ngouela, S., Tsamo, E., Sidhu, N., Dittrich, B., Laatsch, H., 2013. Ingacamerounol, a new flavonol and other chemical constituents from leaves and stem bark of *Inga edulis* Mart. Bull. Kor. Chem. Soc. 34, 3859–3862. https://doi.org/10.5012/bkcs.2013.34.12.3859.

Thuerig, B., Ramseyer, J., Hamburger, M., Oberhänsli, T., Potterat, O., Schärer, H.J., Tamm, L., 2016. Efficacy of a *Juncus effusus* extract on grapevine and apple plants against *Plasmopara viticola* and *Venturia inaequalis*, and identification of the major active constituent. Pest Manag. Sci. 72, 1718–1726. https://doi.org/10.1002/ps.4199.

Wilcox, W., Walter, W., Uyemoto, J., 2015. Front matter. In: Compendium of Grape Diseases, Disorders, and Pests, second ed. APS Publications, St. Paul, MN. https://doi.org/10.1094/9780890544815.fm.

Wolters, B., 1966. The effect of some triterpenes and saponins on fungi. Sci. Nat. = Naturwissenschaften 53, 23.

Zaynab, M., Sharif, Y., Abbas, S., Afzal, M.Z., Qasim, M., Khalofah, A., Ansari, M.J., Khan, K.A., Tao, L., Li, S., 2021. Saponin toxicity as key player in plant defense against pathogens. Toxicon 193, 21–27. https://doi.org/10.1016/j.toxicon.2021.01.009.

Zheng, L., Zheng, J., Zhao, Y., Wang, B., Wu, L., Liang, H., 2006. Three anti-tumor saponins from *Albizia julibrissin*. Bioorg. Med. Chem. Lett 16, 2765–2768. https://doi.org/10.1016/j.bmcl.2006.02.009.

Zou, K., Tong, W.Y., Liang, H., Cui, J.R., Tu, G.Z., Zhao, Y.Y., Zhang, R.Y., 2005. Diastereoisomeric saponins from *Albizia julibrissin*. Carbohydr. Res. 340, 1329–1334. https://doi.org/10.1016/j.carres.2004.10.027.

Zou, K., Zhang, Q.Y., Wang, B., Cui, J.R., Zhao, Y.Y., Zhang, R.Y., 2010. Cytotoxic triterpenoid saponins acetylated with monoterpenoid acid from *Albizia julibrissin*. Helv. Chim. Acta 93, 2100–2106. https://doi.org/10.1002/hlca.201000059.

Zulkifly, A.H., Roslan, D.D., Hamid, A.A.A., Hamdan, S., Huyop, F., 2010. Biodegradation of low concentration of monochloroacetic acid-degrading *Bacillus sp*. TW1 isolated from terengganu water treatment and distribution plant. J. Appl. Sci. 10, 2940–2944. https://doi.org/10.3923/jas.2010.2940.2944.